# Cytokeratin 8 Inhibits Hepatic Glycogen Synthesis in Type 2 Diabetes Mellitus by Modulating Insulin-dependent IRS1/PI3K/Akt-GSK3β Pathway

**Mingzhu Sun** ( sunmingzhu529@126.com )
Endocrinology Department, the second affiliated hospital, Xi'an Jiaotong University
**Jin Sun**
National & Local Joint Engineering Research Center of Biodiagnosis and Biotherapy, the second affiliated hospital
**Zhidong Wang**
General surgery Department, the second affiliated hospital, Xi'an Jiaotong University
**Xiaojuan Quan**
Endocrinology Department, the second affiliated hospital, Xi'an Jiaotong University
**Lin Zhang**
Endocrinology Department, the second affiliated hospital, Xi'an Jiaotong University
**Xiuli Li**
Endocrinology Department, the second affiliated hospital, Xi'an Jiaotong University

**Research Article**

**Keywords:** type 2 diabetes mellitus, hepatic glycogen synthesis, IRS1/PI3K/Akt-GSK3β pathway, Cytokeratin 8

**Posted Date:** June 29th, 2021

**DOI:** https://doi.org/10.21203/rs.3.rs-631811/v1

# Abstract

**Purpose:** Cytokeratin 8(CK8) is a cytoskeletal protein mainly expressed in the liver. Recent studies have found that CK8 was closely related to glycogen synthesis. However, the role and the underlying mechanisms of CK8 in hepatic glycogen synthesis in type 2 diabetes mellitus (T2DM) have remained to be fully elucidated. Therefore, this study aimed to investigate the effects and the underlying mechanisms of CK8 on hepatic glycogen synthesis in T2DM.

**Methods** The T2D mouse model was constructed by high energy feed of 8-10 weeks old C57BL/6J male mice. The model was validated by OGTT test and ITT test. The liver samples of T2DM patients were collected and the expression levels of CK8, IRS1, PI3K, Akt, GSK3β, p-PI3K p-Akt and p-GSK3β were determined by Western blotting. Then, at the cellular level the murine NCTC 1469 cells were used, and to up-regulate and down-regulate the CK8 gene the overexpression plasmid was constructed and transfected and RNA interference technology was applied, and CK8, IRS1, PI3K, Akt, GSK3β, p-IRS1, p-PI3K p-Akt and p-GSK3β were detected by Western blotting. Immunohistochemistry was used to detect the level of glycogen synthase (GS) and glycogen staining experiments was performed by PAS. At the animal level, the T2D mouse model was used to up-regulate and down-regulate the CK8 gene using an adenovirus vector. The levels of CK8, PI3K, Akt, GSK3β, p-PI3K, p-Akt and p-GSK3β in rat liver were detected by Western blotting, immunohistochemistry was used to detect the level of GS and glycogen staining experiments was performed by PAS.

**Results** The expression levels of IRS1, p-PI3K, p-Akt and p-GSK3β were significantly higher, while the expression levels of CK8 was significantly lower in control group than in the liver of T2D mice or T2DM patients. Upregulation of CK8 in murine NCTC 1469 cells treated with high-glucose medium, we found IRS1, p-IRS1, p-PI3K, p-Akt and p-GSK3β were significantly decreased, the level of GS was significantly decreased, and glycogen synthesis was inhibited compared with NCTC1469 cells transfected with empty vector. Downregulation of CK8 in murine NCTC 1469 cells murine treated with high-glucose medium, we found IRS1, p-IRS1, p-PI3K, p-Akt and p-GSK3β were significantly higher, the level of GS was significantly increased, and glycogen synthesis was promoted compared with NCTC1469 cells transfected with sh-NC. Upregulation of CK8 in the T2D mouse model, we found p-PI3K, p-Akt and p-GSK3β were significantly lower compared with T2D mouse model transfected with empty vector. The level of GS was significantly decreased, and glycogen synthesis was inhibited. Downregulation of CK8 in the T2D mouse model, we found p-PI3K, p-Akt and p-GSK3β were significantly increased, and the level of GS was significantly increased, and glycogen synthesis was promoted compared with T2D mouse model transfected with sh-NC.

**Conclusions** Overall, this experiment provides a new molecular target for the treatment of T2DM by revealing the role of CK8 inhibiting hepatic glycogen synthesis in T2DM via regulating insulin-dependent IRS1/PI3K-Akt-GSK3β pathway. CK8 may play an important role in the pathogenesis of glycogen synthesis in T2DM.

# Introduction

Type 2 diabetes mellitus (T2DM), a kind of metabolic disease, is the third leading cause of death worldwide [1]. T2DM is characterized as high levels of blood glucose, which might cause multiple organ injury such as the liver, kidneys, nerves heart and vasculature. According to the reports of WHO (World Health Organization), 422 million people are patients of diabetes mellitus (DM) worldwide and over 90% of adult patients suffer from T2DM [2, 3]. T2DM often accompanied by insulin resistance, β-cell dysfunction and inadequate compensatory response of insulin secretory [4, 5]. It also has been demonstrated that the organs include the liver, pancreas, small intestine, skeletal muscle, brain and kidneys tissue participated in T2DM development [6]. Currently, insulin and synthetic drugs as main types of drugs have been used to the clinical treatment of T2DM. However, these drugs could lead to a number of side-effects such as drug resistance, weight gain and dropsy on T2DM patients [7]. Thus, it is important to develop a new effective target for treatment of T2DM. Numerous studies have demonstrated that multiple mechanisms such as insulin resistance, glycolipids metabolic disorders and inflammation contribute to T2DM development [8-10]. Nevertheless, its molecular mechanism of T2DM development is unclear.

Cytokeratins belong to a subfamily of intermediate filament protein, which often known as structural constituents such as cell cytoskeleton structure [11]. Cytokeratin 8 (CK8) is an important member of cytokeratins and expresses in internal organs, tumors and hepatocytes [12-14]. CK8 has been reported to regulate various physiological processes such as cell differentiation, cell apoptosis, cell protection and multiple drug resistance [15-18]. Recently, a role of CK8 in liver glycogen synthesis has been documented [19]. The IRS1 pathway has been demonstrated to play an important role in T2DM development [20, 21]. The PI3K/AKT-GSK3β pathway as downstream pathway of IRS1 also has been reported to contribute to T2DM development and hepatic glucose output [22-24]. Interestingly, CK8 might regulated of insulin receptor signaling through IRS1/PI3K/Akt-GSK3β pathway in hepatocytes [25]. All data suggest that CK8 and IRS1/PI3K/Akt-GSK3β pathway may play a role in regulating liver glycogen synthesis of T2DM. However, the relationship among CK8, IRS1/PI3K/AKT-GSK3βpathway and glycogen synthesis has not been reported.

In this study, we attempted to explore the mechanism of CK8-mediated IRS1/PI3K/AKT-GSK3β pathway in hepatic glycogen synthesis of T2DM. A T2DM mice model and high-glucose NCTC 1469 cell model are used to determine whether CK8 and the IRS1/PI3K/AKT-GSK3β pathway are contribute to liver glycogen synthesis of T2DM and further revealed its molecular mechanisms. These findings may provide a new potential approach to enhance hepatic glycogen synthesis of T2DM.

# Materials And Methods

### Reagents and antibody

The anti-IRS1, anti-P-IRS1, anti-PI3K, anti-P-PI3K, anti-P-AKT, anti-AKT, anti- GSK3β, anti-p-GSK3β, anti-glycogen synthase (GS), anti-CK8 and anti-GAPDH were purchased from Cell Signal Technology. Dulbecco's modified Eagle's medium (DMEM) medium, horse serum (HS), penicillin and streptomycin were obtained from Procell (Wuhan, Hubei, China).

## Patient samples

The liver tissue samples of normal Subjects and patient with type 2 diabetes mellitus and were collected from March 2020 to October 2020 in The Second Affiliated Hospital of Xi'an Jiaotong University. All participants provided written informed consents, and the study was approved by the Ethical Committee of The Second Affiliated Hospital of Xi'an Jiaotong University.

## Cell culture and treatment

The mouse NCTC 1469 hepatocytes were purchased from Procell (Wuhan, Hubei, China). Cells were maintained in DMEM (Dulbecco's modified Eagle's medium) supplemented with 10% HS (horse serum), 100 μg/mL streptomycin and 100 U/ml penicillin at 37 °C in a humidified incubator under an atmosphere of 95% air and 5% $CO_2$. The mouse NCTC 1469 hepatocytes were grown to 70%-80% cell confluence and exposed to normal glucose (5.5 m mmol/L) or high glucose (33.3 mmol/L) for 24 hours.

## Oral Glucose Tolerance Test (OGTT) and Insulin Tolerance Test (ITT)

The OGTT and ITT were performed after a high-fat diet C57BL/6J mice on week 14. C57BL/6J mice were fasted overnight and treated with 2.0 g/kg D-glucose by oral gavage. Blood glucose level was detected at 0, 15, 30, 90 and 120 min after the glucose administration for OGTT. C57BL/6J mice were fasted for 4 h and injected intraperitoneally with 0.75 U/kg insulin. Blood glucose level was detected at 0, 15, 30, 45 and 60 min after the insulin administration for ITT.

## Establishment animal models

Eighteen C57BL/6J male mice (8 weeks old) were purchased from Biofavor Ltd. (Wuhan, China) and used in this study. All mice were maintained in an animal room (22±2°C, 50% ± 5% humidity and 12-h light/12-h dark cycle) for 1 week of adaptation before the experiment. All animal experiments were approved by The Committee on Ethical Use of Animals of The Second Affiliated Hospital of Xi'an Jiaotong University. After one week of adaptive, eighteen C57BL/6J male mice were randomly divided into six groups (n=3 in each group): A. normal group: mice were fed with normal diets for 12 weeks. B. DM group: mice were fed with high-fat diets for 12 weeks. C. DM transfected with CK8 group: mice were injected with $1X10^7$pfu adenovirus (Ad-ZsGreen-CK8, each mouse) once a week were fed with high-fat diets for 12 weeks. D. DM transfected with empty vector group: mice were injected with $1X10^7$pfu adenovirus (Ad-ZsGreen-vector, each mouse) once a week were fed with high-fat diets for 12 weeks. E. DM transfected with shRNA-CK8 group: mice were injected with $1X10^7$pfu adenovirus (Ad-ZsGreen-shRNA-CK8, each mouse) once a week were fed with high-fat diets for 12

weeks. F. DM transfected with shRNA-NC group: mice were injected with $1X10^7$pfu adenovirus (Ad-ZsGreen-shRNA-NC, each mouse) once a week were fed with high-fat diets for 12 weeks. Then, all DM groups were injected with 30 mg/kg STZ and normal group was injected with a buffer solution for four days in a row. FBG levels ≥11.1 mM was considered as establishment of T2DM mice model.

### Determination of insulin levels

The serum was collected from C57BL/6J mice and insulin levels were detected by Mouse Insulin ELISA Kit Beyotime Biotech, China) following the manufacturer's instructions. Each sample were performed in triplicate, and the absorbance at 450 nm was examined with Multiskan MK3 (Thermo Fisher Scientific, Inc, Waltham, MA, USA).

### Immunohistochemistry staining

The liver tissue specimens were dehydrated in graded concentrations of ethanol and then embedded in paraffin. The specimens were cut into a thickness of 4 μm section. After dewaxing, rehydration and blocking, the thick tissue slides (4 μm) were incubated with anti- glycogen synthase at 4°C for 60 min, and then incubated with Dako REAL EnVision Detection system at room temperature for 30 min and the slides were counterstained with Mayer's hematoxylin. After the last wash, the slides were observed using an inverted microscope (BX53, Olympus, Tokyo, Japan).

The mouse NCTC 1469 hepatocytes were seeded at a density of $3\times10^4$ cells on a cover slip and incubated at 37°C overnight. Then, the medium was removed and cells were fixed using 4% paraformaldehyde and permeabilized using 0.5% Triton at room temperature. After three times wash, cover slip was incubated with anti- glycogen synthase at 4°C for 60 min, and then incubated with Dako REAL EnVision Detection system at room temperature for 30 min and the slides were counterstained with Mayer's hematoxylin. After the last wash, the cover slips were observed using a inverted microscope (BX53, Olympus, Tokyo, Japan).

### PAS staining

Hepatic glycogen was examined using PAS staining. The liver tissue specimens were dehydrated in graded concentrations of ethanol and then embedded in paraffin. The specimens were cut into a thickness of 4 μm section. After dewaxing and rehydration, the thick tissue slides (4 μm) were stained with PAS reagent. After the last wash, the slides were observed using an inverted microscope (BX53, Olympus, Tokyo, Japan).

The mouse NCTC 1469 hepatocytes were seeded at a density of $3\times10^4$ cells on a cover slip and incubated at 37°C overnight. Then, the medium was removed and cells were fixed using 4% paraformaldehyde and permeabilized using 0.5% Triton at room temperature. After three times wash, cover slips were stained with PAS reagent and were observed using an inverted microscope (BX53, Olympus, Tokyo, Japan).

### Plasmids

The coding region sequences of mouse CK8 were amplified by PCR (forward: 5'-CTAGCTAGCCACCATGTCCATCAGGGTGACTCAGAAAT-3', reverse: 5'-CCCAAGCTTTCACTTGGACACGACATCAGAAGACTCG-3'). The cDNA of mouse CK8 were cloned into pDC316-mCMV-ZsGreen. The mouse CK8 siRNA sequence (5'-CCAUGUACCAGAUUAAGUA-3') was constructed. Antisense CK8 cDNA was inserted into the adenoviral plasmids pDC316-ZsGreen-shRNA using two cDNA primers (5'- CCGGCCATGTACCAGATTAAGTATTCAAGAGATACTTAATCTGGTACATGGTTTTTTG -3' and 5'- GATCCAAAAAACCATGTACCAGATTAAGTATCTCTTGAATACTTAATCTGGTACATGG -3'). The siRNA-NC sequence (5'- UUCUCCGAACGUGUCACGU -3') was constructed. Antisense siRNA-NC cDNA was inserted into the adenoviral plasmids pDC316-ZsGreen-shRNA using two cDNA primers (5'- CCGGTTCTCCGAACGTGTCACGTTTCAAGAGAACGTGACACGTTCGGAGAATTTTTTG -3' and 5'- GATCCAAAAAATTCTCCGAACGTGTCACGTTCTCTTGAAACGTGACACGTTCGGAGAA -3').

### Western blot analysis

The related proteins expression was performed using western blot analysis as previously described [26, 27]. Briefly, NCTC 1469 hepatocytes or liver tissue samples were collected and lysed in RIPA lysis buffer (Beyotime, Nantong, Jiangsu, China) containing 1 % protease inhibitors cocktail (Sigma, Saint Louis, MO, USA). The protein lysates were resolved by electrophoresis on SDS-PAGE and transferred to nitrocellulose membranes (Mllipore, USA). After blocking with5% nonfat milk, the membranes were incubated with primary antibodies against IRS1 (1:2000), P-IRS1 (1:1000), PI3K (1:2000), P-PI3K (1:1000), P-AKT (1:1000), AKT (1:2000), P-GSK3β (1:3000), p-GSK3β (1:3000), CK8 (1:2000) and GAPDH (1:4000) at 4 °C overnight. Then, nitrocellulose membranes were treated with HRP-conjugated secondary antibodies (1:2000) for 2 h at room temperature and a hypersensitive ECL chemiluminescence reagent (Beyotime Institute of Biotechnology) was used to detect the signal of the immunoreactive bands.

### Statistical analysis

All results were carried out in triplicates and expressed as mean ± SD. Statistical analysis was done by one-way ANOVA followed by Dunnett’s test and Student's t test with GraphPad Prism 7.0 software. $P < 0.05$ was considered statistically significant.

## Results

### CK8 expression was upregulated in the liver tissue samples of T2DM patient

We firstly examined the liver glycogen content in the liver tissue of T2DM patient and normal human subjects by using PAS staining. As shown in Fig 1A, the liver glycogen content was markedly decreased in T2DM patient compared with normal human subjects. We further detected the expression of CK8 protein in the liver tissue of T2DM patient and normal human subjects by western blot analysis. Our results

demonstrated that CK8 protein was significantly increased in T2DM patient compared with normal human subjects (Fig 1B and 1C). These data indicated that CK8 protein might involve in the regulation of liver glycogen synthesis in T2DM patient.

### The IRS1/PI3K/AKT-GSK3β pathway was inhibited in the liver tissue samples of T2DM patient

Western blot analysis was conducted to detected the expression level of IRS1 protein in the liver tissue of T2DM patient and normal human subjects. As shown in Figure 2 A and 2B, the level expression of IRS1 protein was significantly downregulated in T2DM patient compared with normal human subjects. Furthermore, the expression levels of PI3K and AKT protein as well as the extent of PI3K and AKT phosphorylation were performed by western blot analysis in the liver tissue of T2DM patient and normal human subjects. We observed that PI3K and AKT phosphorylation were significantly deceased, while the levels of PI3K and AKT protein were no significantly changed in the liver tissue of T2DM patient and normal human subjects (Figure 2 A, 2C and 2D). We also examined the expression levels of GSK3β, phosphorylation of GSK3β and GS protein by using western blot analysis and immunohistochemistry staining. In comparison with normal human subjects, GS and phosphorylation of GSK3β phosphorylation were significantly deceased, while the level of GSK3β protein was significantly no changed in the liver tissue of T2DM patient and normal human subjects (Figure 3A-3D). These results suggested that IRS1/PI3K/AKT pathway might play a role in liver glycogen synthesis in T2DM patient.

### High-glucose treatment upregulated CK8 expression and inhibited IRS1/PI3K/AKT-GSK3β pathway in liver cell line NCTC1469

Further experiments were performed to explore the effect high-glucose on CK8 expression and IRS1/PI3K/AKT pathway in liver cell line NCTC1469. As shown in Figure 4A, high-glucose treatment markedly decreased glycogen content of NCTC1469 cells. Compared with normal glucose group, high-glucose treatment significantly inhibited the expression levels of IRS1 and phosphorylation of IRS1, PI3K, AKT and GSK3β were significantly deceased, while CK8 was significantly increased after high-glucose treatment in NCTC1469 cells. Interestingly, the levels of PI3K, AKT and GSK3β protein was significantly no changed in high-glucose group compared with normal glucose group (Figure 4B). Besides, immunohistochemistry staining revealed that high-glucose significantly reduced the expression levels of GS compared with normal glucose group in NCTC1469 cells (Figure 4I and 4J). These findings demonstrated that CK8 and IRS1/PI3K/AKT-GSK3β pathway might participate in glycogen synthesis of NCTC1469 cells.

### CK8 suppressed glycogen synthesis via inhibiting IRS1/PI3K/AKT-GSK3β pathway in NCTC1469 cells

To determine the relationship among CK8, IRS1/PI3K/AKT-GSK3β pathway and glycogen synthesis, we explored the effects of CK8 on glycogen synthesis and IRS1/PI3K/AKT-GSK3βpathway in NCTC1469 cells. Firstly, glycogen content was examined by using PAS staining in NCTC1469 cells. Compared with NCTC1469 cells transfected with empty vector and incubated with high-glucose medium, overexpress CK8 markedly decreased glycogen content of NCTC1469 cells treated with high-glucose

medium (Figure 5A). Knockdown of CK8 markedly increased glycogen content of NCTC1469 cells compared with NCTC1469 cells transfected with sh-NC (Figure 5A). Furthermore, overexpresses CK8 significantly downregulated the IRS1 and phosphorylation of IRS1, PI3K, AKT and GSK3β protein in compared with NCTC1469 cells transfected with empty vector (Figure 5B-5H). Compared with NCTC1469 cells transfected with sh-NC, knockdown of CK8 significantly upregulated the IRS1 and phosphorylation of IRS1, PI3K, AKT and GSK3β protein in high-glucose treated NCTC1469 cells (Figure 5B-5H). However, PI3K, AKT and GSK3β protein expression levels were significantly no changed in all NCTC1469 cells groups (Figure 5B). Additionally, overexpresses CK8 significantly reduced GS protein expression level, while knockdown of CK8 significantly increased GS protein expression level in high-glucose treated NCTC1469 cells (Figure 5I and 5J). These results suggested that CK8 might participate in glycogen synthesis of NCTC1469 cells via regulating IRS1/PI3K/AKT-GSK3β pathway.

### CK8 suppressed glycogen synthesis via inhibiting PI3K/AKT-GSK3β pathway in T2DM mice

We further explored the relationship among CK8, PI3K/AKT-GSK3β pathway and glycogen synthesis in T2DM mice model. The insulin level of the blood serum was detected by using ELISA assay in T2DM mice and control mice. As shown in Figure 6A, the insulin level of the blood serum was significantly increased in T2DM mice compared with control mice (Figure 6A). We furthermore observed glucose metabolism in T2DM mice and control mice by OGTT and ITT. The glucose level of blood was significantly increased after the oral injection of glucose in T2DM mice compared with control mice (Figure 6B). The glucose level of blood was also significantly increased after injection with insulin in T2DM mice compared with control mice (Figure 6C). PAS staining analysis revealed that the liver glycogen content of mice was also markedly decreased in T2DM mice compared with control mice (Figure 6D). Overexpress CK8 also was markedly decreased the liver glycogen content of T2DM mice compared with T2DM mice transfected with empty vector (Figure 6D). Compared with T2DM mice transfected with sh-NC, knockdown of CK8 markedly increased the liver glycogen content of T2DM mice (Figure 6D). PI3K/AKT pathway was examined by western blot analysis in T2DM mice and control mice. We found that phosphorylation of PI3K, AKT and GSK3β protein were downregulated in T2DM mice, while CK8 were upregulated in T2DM mice compared with control mice (Figure 6E). Overexpresses CK8 reduced phosphorylation of PI3K, AKT and GSK3β protein in compared with T2DM mice transfected with empty vector (Figure 6E). Compared with T2DM mice transfected with sh-NC, knockdown of CK8 upregulated phosphorylation of PI3K, AKT and GSK3β protein in T2DM mice (Figure 6E). However, PI3K, AKT and GSK3β protein expression levels were significantly no changed in all mice groups (Figure 6E). These results indicated that CK8 might participate in glycogen synthesis of T2DM mice via regulating PI3K/AKT-GSK3β pathway.

## Discussion

In the present study, we observed that CK8 was upregulated and glycogen content was reduced in the liver tissue of T2DM patient. We also found that CK8 was increased and glycogen content was decreased in high glucose-incubated NCTC1469 cells and T2DM mice. Furthermore, we observed that

IRS1/PI3K/AKT pathway, GS protein and phosphorylation of GSK3β protein were decreased in the liver tissue of T2DM patient and high glucose-incubated NCTC1469 cells. In T2DM mice, IRS1/PI3K/AKT-GSK3βsignaling pathway also was inhibited. Additionally, overexpress CK8 inhibited IRS1/PI3K/AKT-GSK3βsignaling pathway and reduced glycogen content in the liver tissue of T2DM patient and high glucose-incubated NCTC1469 cells. Knockdown of CK8 activated IRS1/PI3K/AKT-GSK3β signaling pathway and increased glycogen content in the liver tissue of T2DM patient and high glucose-incubated NCTC1469 cells.

IRS1 was known as insulin receptor substrate 1, which played important role in regulating cell such as cell proliferation, cell apoptosis, cell metabolism [24, 28, 29]. IRS1 also widely distributed in insulin sensitive tissues and closely related to insulin signaling [30, 31]. It has been reported that IRS-1 genetic polymorphism was closely associated with insulin resistance [32, 33]. Xu et al. have demonstrated that Angptl7 mediated insulin resistance and T2DM by inhibiting the IRS1 expression through SOCS3 [20]. *Wushenziye* Formula improved insulin resistance in skeletal muscle cell of T2DM by increasing phosphorylation of IRS1 [21]. Our results showed that IRS1 was significantly downregulated in the liver tissue of T2DM patient. IRS1 and phosphorylation of IRS1 also was markedly reduced in high glucose-incubated NCTC 1469 cells and the liver tissue of T2DM mice. Furthermore, numerous studies have demonstrated that PI3K/AKT pathway was associated with insulin resistance in T2DM [34-36]. It also been reported that IRS1 played a vital role in regulating PI3K/AKT pathway in a variety of cells [24, 37, 38]. Guo et al. have reported that Panax notoginseng saponins improved significantly glucose tolerance and insulin tolerance in skeletal muscle by PI3K/AKT pathway through IRS1 [39]. Our results suggested that phosphorylation of PI3K and AKT were significantly inhibited in the liver tissue of T2DM patient, high glucose-incubated NCTC 1469 cells and the liver tissue of T2DM mice. Additionally, in HepG2 cells, Akt might regulate glycogen metabolism through GSK3β and GS [40]. Chloroquine might increase glucose uptake via regulating AKT-mediated activation of GS in muscle cells [41]. We found the glycogen content was markedly in the liver tissue of T2DM patient, high glucose-incubated NCTC 1469 cells and the liver tissue of T2DM mice. GS and phosphorylation of GSK3β was reduced in the liver tissue of T2DM patient and high glucose-incubated NCTC 1469 cells. We also observed that phosphorylation of GSK3β was decreased in the liver tissue of T2DM mice. All data indicated IRS1/PI3K/AKT-GSK3β pathway participated in regulation of hepatic glycogen synthesis in T2DM.

CK8, a kind of intermediate filament protein, has been documented to involved in regulating multiple cellular functions such as cell differentiation, cell apoptosis and cell protection [15-17]. Recent studies have found that CK8 plays an important role in regulating glycogen synthesis and glucose metabolism. Alam et al. has demonstrated that CK8 was upregulated in islets of mice in high glucose condition and knockdown of CK8 decreased fasting blood glucose and increased glucose tolerance and insulin sensitivity [42]. Mathew et al. also has reported that knockdown of CK8 enhanced insulin-stimulated glycogen formation in normal and cancerous hepatic cells [19]. Our results showed that CK8 was increased in the liver tissue of T2DM patient, high glucose-incubated NCTC 1469 cells and the liver tissue of T2DM mice. Overexpress CK8 also was markedly decreased glycogen content in the liver tissue of T2DM patient, high glucose-incubated NCTC 1469 cells and the liver tissue of T2DM mice. knockdown

of CK8 was significantly increased glycogen content in the liver tissue of T2DM patient, high glucose-incubated NCTC 1469 cells and the liver tissue of T2DM mice. Moreover, CK8 might regulated of insulin receptor signaling and trafficking via IRS1/PI3K/Akt pathway and Rab5 in hepatocytes [25]. Our results demonstrated overexpress CK8 significantly inhibited IRS1/PI3K/AKT-GSK3βpathway in the liver tissue of T2DM patient, high glucose-incubated NCTC 1469 cells and the liver tissue of T2DM mice. Additionally, knockdown of CK8 was significantly activated IRS1/PI3K/AKT-GSK3β pathway in the liver tissue of T2DM patient, high glucose-incubated NCTC 1469 cells and the liver tissue of T2DM mice. These finding suggested CK8 regulated liver glycogen synthesis in type 2 diabetes mellitus through IRS1/PI3K/AKT-GSK3β pathway.

In general, our study suggested that CK8 was unregulated in liver tissue of T2DM patient. CK8 might reduce hepatic glycogen synthesis in T2DM patient through inhibiting IRS1/PI3K/AKT-GSK3β pathway. Our findings will provide a new potential therapeutic target for T2DM patient.

# Declarations


### Acknowledgements

Not applicable.

### Funding

This work was financially supported by the National Natural Science Foundation of Shaanxi Province (2019JQ-968) and the Key project of Natural Science Foundation of Shaanxi Province (2021JZ-38).


### Availability of data and materials

The datasets used and/or analyzed during the present study are available from the corresponding author on reasonable request.

### Authors' contributions

SMZ conducted the experiments and analyzed the data. SMZ and LXL made substantial contributions to the design of the present study and prepared the manuscript. SJ, WZD, QXJ and ZL performed the western blotting and analyzed the data. All authors read and approved the final manuscript.

### Ethics approval and consent to participate

The liver tissue samples of normal Subjects and patient with type 2 diabetes mellitus and were collected from March 2020 to October 2020 in The Second Affiliated Hospital of Xi'an Jiaotong University. All participants provided written informed consents, and the study was approved by the Ethical Committee of The Second Affiliated Hospital of Xi'an Jiaotong University.

### Conflict of interests

The authors declare that they have no competing interests.

# References


[1] Y. Liu, J. Deng, D. Fan, Ginsenoside Rk3 ameliorates high-fat-diet/streptozocin induced type 2 diabetes mellitus in mice via the AMPK/Akt signaling pathway, Food & function 10(5) 2538-2551 (2019).

[2] J. Compston, Type 2 diabetes mellitus and bone, Journal of internal medicine 283(2) 140-153 (2018).

[3] N. Holman, B. Young, R. Gadsby, Current prevalence of Type 1 and Type 2 diabetes in adults and children in the UK, Diabetic medicine : a journal of the British Diabetic Association 32(9) 1119-20. (2015)

[4] M. Stumvoll, B.J. Goldstein, T.W. van Haeften, Type 2 diabetes: principles of pathogenesis and therapy, Lancet 365(9467) 1333-46 (2005).

[5] C. Weyer, C. Bogardus, D.M. Mott, R.E. Pratley, The natural history of insulin secretory dysfunction and insulin resistance in the pathogenesis of type 2 diabetes mellitus, The Journal of clinical investigation 104(6) 787-94 (1999).

[6] R.A. Defronzo, Banting Lecture. From the triumvirate to the ominous octet: a new paradigm for the treatment of type 2 diabetes mellitus, Diabetes 58(4) 773-95 (2009).

[7] J.M. Pappachan, C.J. Fernandez, E.C. Chacko, Diabesity and antidiabetic drugs, Molecular aspects of medicine 66  3-12 (2019).

[8] J. Ji, C. Zhang, X. Luo, L. Wang, R. Zhang, Z. Wang, D. Fan, H. Yang, J. Deng, Effect of Stay-Green Wheat, a Novel Variety of Wheat in China, on Glucose and Lipid Metabolism in High-Fat Diet Induced Type 2 Diabetic Rats, Nutrients 7(7) 5143-55 (2015).

[9] S. Sharma, R. Taliyan, Histone deacetylase inhibitors: Future therapeutics for insulin resistance and type 2 diabetes, Pharmacological research 113(Pt A) 320-326 (2016).

[10] B. Zhang, Q. Shen, Y. Chen, R. Pan, S. Kuang, G. Liu, G. Sun, X. Sun, Myricitrin Alleviates Oxidative Stress-induced Inflammation and Apoptosis and Protects Mice against Diabetic Cardiomyopathy, Scientific reports 7  44239 (2017).

[11] P. Dey, J. Togra, S. Mitra, Intermediate filament: structure, function, and applications in cytology, Diagnostic cytopathology 42(7) 628-35 (2014).

[12] R. Moll, W.W. Franke, D.L. Schiller, B. Geiger, R. Krepler, The catalog of human cytokeratins: patterns of expression in normal epithelia, tumors and cultured cells, Cell 31(1) 11-24 (1982).

[13] W.W. Franke, H. Denk, R. Kalt, E. Schmid, Biochemical and immunological identification of cytokeratin proteins present in hepatocytes of mammalian liver tissue, Experimental cell research 131(2) 299-318

(1981).

[14] R.A. Quinlan, J.A. Cohlberg, D.L. Schiller, M. Hatzfeld, W.W. Franke, Heterotypic tetramer (A2D2) complexes of non-epidermal keratins isolated from cytoskeletons of rat hepatocytes and hepatoma cells, Journal of molecular biology 178(2) 365-88 (1984).

[15] I.A.K. Lähdeniemi, J.O. Misiorek, C.J.M. Antila, S.K. Landor, C.A. Stenvall, L.E. Fortelius, L.K. Bergström, C. Sahlgren, D.M. Toivola, Keratins regulate colonic epithelial cell differentiation through the Notch1 signalling pathway, Cell death and differentiation 24(6) 984-996 (2017).

[16] A.T. Lau, J.F. Chiu, The possible role of cytokeratin 8 in cadmium-induced adaptation and carcinogenesis, Cancer research 67(5) 2107-13 (2007).

[17] W.P. Bozza, Y. Zhang, B. Zhang, Cytokeratin 8/18 protects breast cancer cell lines from TRAIL-induced apoptosis, Oncotarget 9(33) 23264-23273 (2018).

[18] F. Liu, Z. Chen, J. Wang, X. Shao, Z. Cui, C. Yang, Z. Zhu, D. Xiong, Overexpression of cell surface cytokeratin 8 in multidrug-resistant MCF-7/MX cells enhances cell adhesion to the extracellular matrix, Neoplasia 10(11) 1275-84 (2008).

[19] J. Mathew, A. Loranger, S. Gilbert, R. Faure, N. Marceau, Keratin 8/18 regulation of glucose metabolism in normal versus cancerous hepatic cells through differential modulation of hexokinase status and insulin signaling, Experimental cell research 319(4) 474-86 (2013).

[20] T. Xu, L. Xu, P. Meng, X. Ma, X. Yang, Y. Zhou, M. Feng, Angptl7 promotes insulin resistance and type 2 diabetes mellitus by multiple mechanisms including SOCS3-mediated IRS1 degradation, FASEB journal : official publication of the Federation of American Societies for Experimental Biology 34(10) 13548-13560 (2020).

[21] C. Tian, H. Chang, X. La, J.A. Li, Wushenziye Formula Improves Skeletal Muscle Insulin Resistance in Type 2 Diabetes Mellitus via PTP1B-IRS1-Akt-GLUT4 Signaling Pathway, Evidence-based complementary and alternative medicine : eCAM 2017 4393529 (2017).

[22] S.H. Chen, X.N. Liu, Y. Peng, MicroRNA-351 eases insulin resistance and liver gluconeogenesis via the PI3K/AKT pathway by inhibiting FLOT2 in mice of gestational diabetes mellitus, Journal of cellular and molecular medicine 23(9) 5895-5906 (2019).

[23] T.Y. Liu, C.X. Shi, R. Gao, H.J. Sun, X.Q. Xiong, L. Ding, Q. Chen, Y.H. Li, J.J. Wang, Y.M. Kang, G.Q. Zhu, Irisin inhibits hepatic gluconeogenesis and increases glycogen synthesis via the PI3K/Akt pathway in type 2 diabetic mice and hepatocytes, Clinical science 129(10) 839-50 (2015).

[24] Z. Cheng, C. Luo, Z. Guo, LncRNA-XIST/microRNA-126 sponge mediates cell proliferation and glucose metabolism through the IRS1/PI3K/Akt pathway in glioma, Journal of cellular biochemistry 121(3) 2170-2183 (2020).

[25] A. Roux, A. Loranger, J.N. Lavoie, N. Marceau, Keratin 8/18 regulation of insulin receptor signaling and trafficking in hepatocytes through a concerted phosphoinositide-dependent Akt and Rab5 modulation, FASEB journal : official publication of the Federation of American Societies for Experimental Biology 31(8) 3555-3573 (2017).

[26] Y. Liu, X. Kang, G. Niu, S. He, T. Zhang, Y. Bai, Y. Li, H. Hao, C. Chen, Z. Shou, B. Li, Shikonin induces apoptosis and prosurvival autophagy in human melanoma A375 cells via ROS-mediated ER stress and p38 pathways, Artificial cells, nanomedicine, and biotechnology 47(1) 626-635 (2019).

[27] X. Kang, H. Wang, Y. Li, Y. Xiao, L. Zhao, T. Zhang, S. Zhou, X. Zhou, Y. Li, Z. Shou, C. Chen, B. Li, Alantolactone induces apoptosis through ROS-mediated AKT pathway and inhibition of PINK1-mediated mitophagy in human HepG2 cells, Artificial cells, nanomedicine, and biotechnology 47(1) 1961-1970 (2019).

[28] A. Ijaz, S. Babar, S. Sarwar, S.U. Shahid, Shabana, The combined role of allelic variants of IRS-1 and IRS-2 genes in susceptibility to type2 diabetes in the Punjabi Pakistani subjects, Diabetology & metabolic syndrome 11 64 (2019).

[29] Y. Jiang, Q. Zhang, C. Soderland, J.J. Steinle, TNFα and SOCS3 regulate IRS-1 to increase retinal endothelial cell apoptosis, Cellular signalling 24(5) 1086-92 (2012).

[30] X.J. Sun, P. Rothenberg, C.R. Kahn, J.M. Backer, E. Araki, P.A. Wilden, D.A. Cahill, B.J. Goldstein, M.F. White, Structure of the insulin receptor substrate IRS-1 defines a unique signal transduction protein, Nature 352(6330) 73-7 (1991).

[31] Q. Yang, T.E. Graham, N. Mody, F. Preitner, O.D. Peroni, J.M. Zabolotny, K. Kotani, L. Quadro, B.B. Kahn, Serum retinol binding protein 4 contributes to insulin resistance in obesity and type 2 diabetes, Nature 436(7049) 356-62 (2005).

[32] A.A. Yousef, E.G. Behiry, W.M.A. Allah, A.M. Hussien, A.A. Abdelmoneam, M.H. Imam, D.M. Hikal, IRS-1 genetic polymorphism (r.2963G>A) in type 2 diabetes mellitus patients associated with insulin resistance, The application of clinical genetics 11 99-106 (2018).

[33] A.A. Albegali, M. Shahzad, S. Mahmood, M.I. Ullah, Genetic association of insulin receptor substrate-1 (IRS-1, rs1801278) gene with insulin resistant of type 2 diabetes mellitus in a Pakistani population, Molecular biology reports 46(6) 6065-6070 (2019).

[34] M. Lee, H. Li, H. Zhao, M. Suo, D. Liu, Effects of Hydroxysafflor Yellow A on the PI3K/AKT Pathway and Apoptosis of Pancreatic β-Cells in Type 2 Diabetes Mellitus Rats, Diabetes, metabolic syndrome and obesity : targets and therapy 13 1097-1107 (2020).

[35] S. Bathina, U.N. Das, Dysregulation of PI3K-Akt-mTOR pathway in brain of streptozotocin-induced type 2 diabetes mellitus in Wistar rats, Lipids in health and disease 17(1) 168 (2018).

[36] T. Imai, T. Sato, H. Arii, T. Fujita, [Influence of anesthesia and surgery upon complement titers in surgical patients (author's transl)], Masui. The Japanese journal of anesthesiology 29(5) 436-41 (1980).

[37] L. Mi, Y. Chen, X. Zheng, Y. Li, Q. Zhang, D. Mo, G. Yang, MicroRNA-139-5p Suppresses 3T3-L1 Preadipocyte Differentiation Through Notch and IRS1/PI3K/Akt Insulin Signaling Pathways, Journal of cellular biochemistry 116(7) 1195-204 (2015).

[38] Y.L. Cao, D.J. Liu, H.G. Zhang, MiR-7 regulates the PI3K/AKT/VEGF pathway of retinal capillary endothelial cell and retinal pericytes in diabetic rat model through IRS-1 and inhibits cell proliferation, European review for medical and pharmacological sciences 22(14) 4427-4430 (2018).

[39] X. Guo, W. Sun, G. Luo, L. Wu, G. Xu, D. Hou, Y. Hou, X. Guo, X. Mu, L. Qin, T. Liu, Panax notoginseng saponins alleviate skeletal muscle insulin resistance by regulating the IRS1-PI3K-AKT signaling pathway and GLUT4 expression, FEBS open bio 9(5) 1008-1019 (2019).

[40] S. Varma, A. Shrivastav, S. Changela, R.L. Khandelwal, Long-term effects of rapamycin treatment on insulin mediated phosphorylation of Akt/PKB and glycogen synthase activity, Experimental cell research 314(6) 1281-91 (2008).

[41] M.J. Halaby, B.K. Kastein, D.Q. Yang, Chloroquine stimulates glucose uptake and glycogen synthase in muscle cells through activation of Akt, Biochemical and biophysical research communications 435(4) 708-13 (2013).

[42] C.M. Alam, J.S.G. Silvander, T.O. Helenius, D.M. Toivola, Decreased levels of keratin 8 sensitize mice to streptozotocin-induced diabetes, Acta physiologica 224(2) e13085 (2018).

# Figures

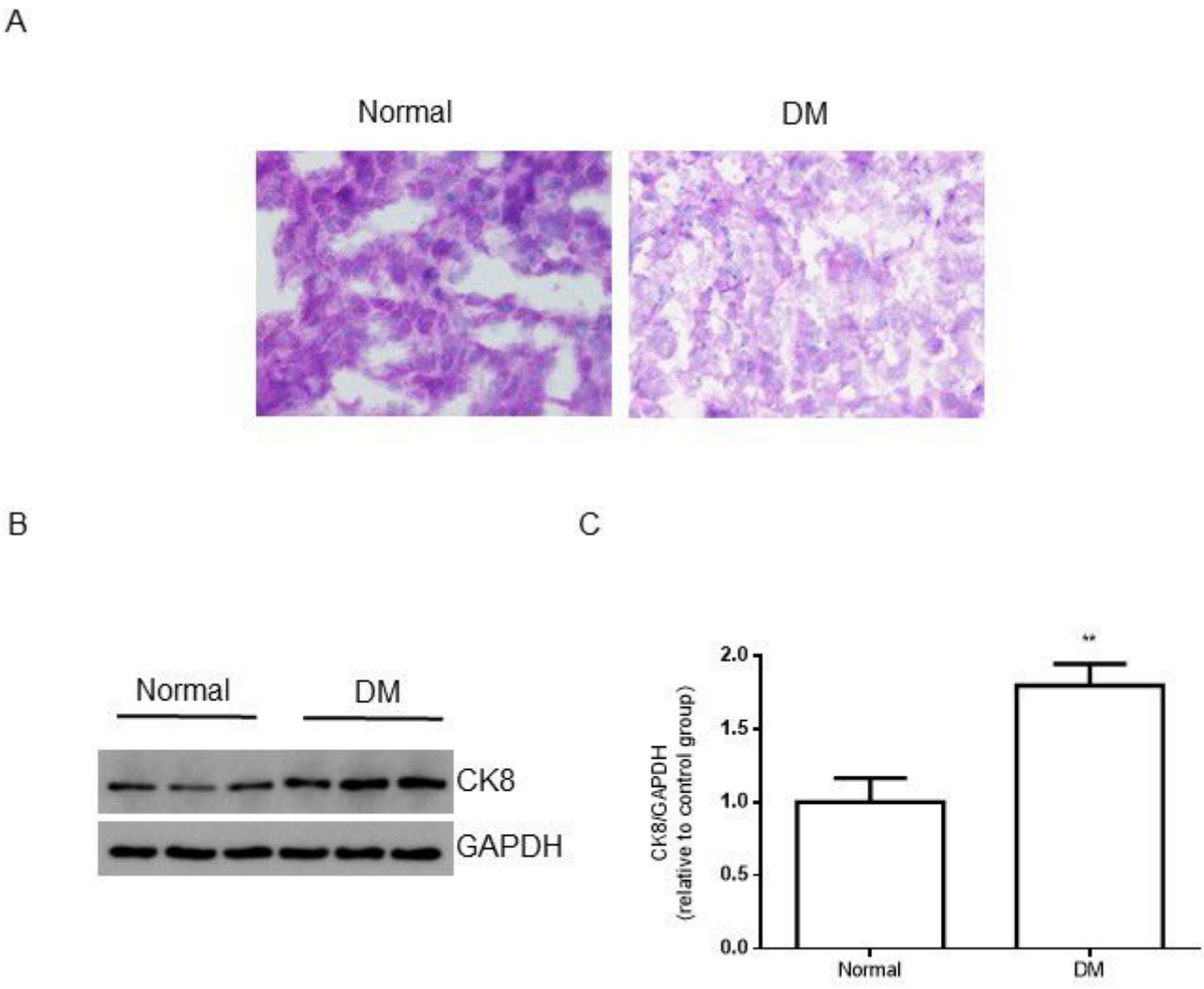


## Figure 1

The of profiles CK8 and liver glycogen synthesis in the liver tissue of T2DM patient and normal human subjects. A. The liver glycogen content was performed by PAS staining in the liver tissue of T2DM patient and normal human subjects (n=3 in each group). B. The expression level of CK8 was determined by Western blot analysis in the liver tissue of T2DM patient and normal human subjects (n=3 in each group). GAPDH was used as the internal control. C. The quantification of CK8 expression. **P < 0.01

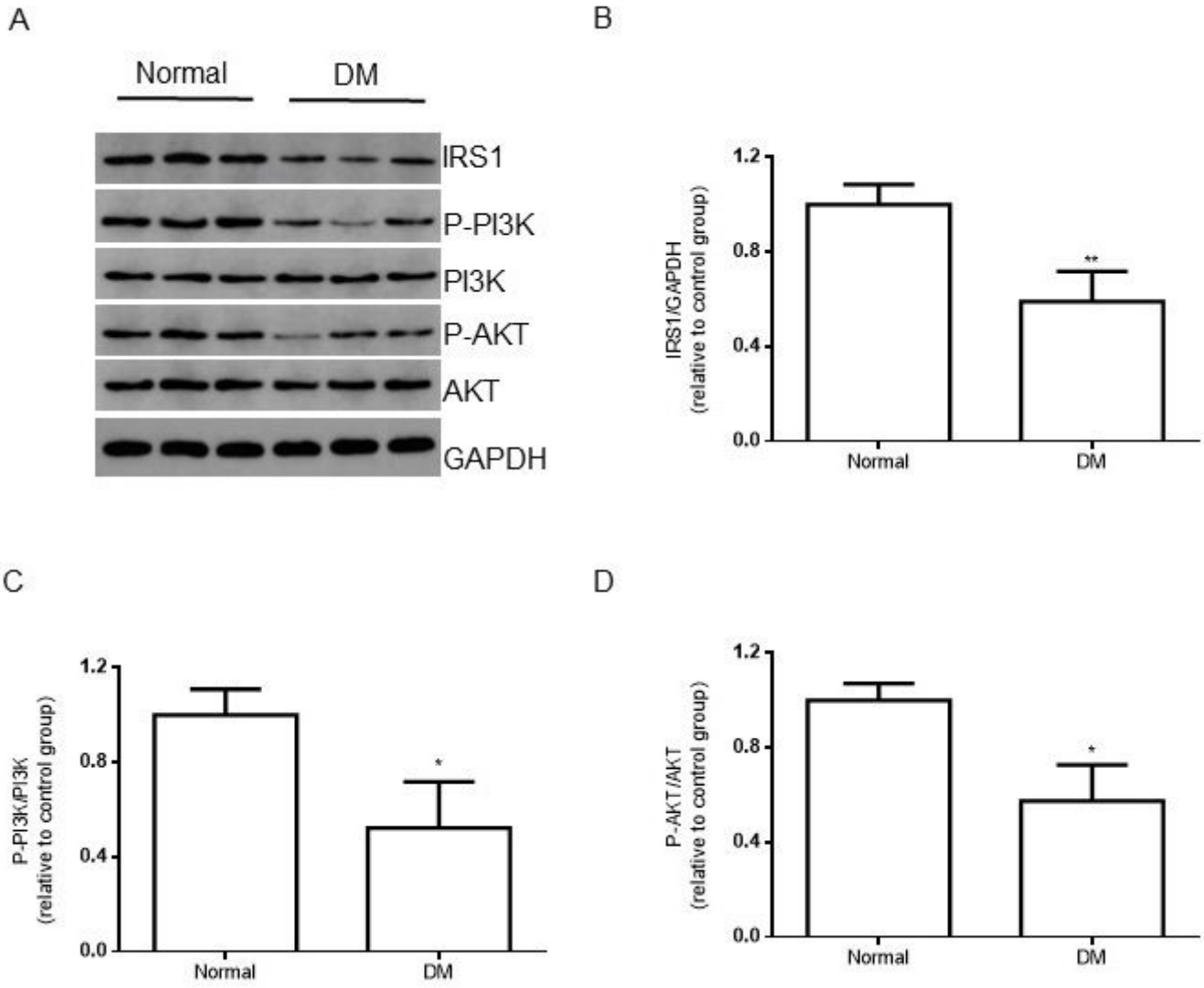


## Figure 2

The expression levels of IRS1, P-PI3K, PI3K, AKT and P-AKT in the liver tissue of T2DM patient and normal human subjects. A. IRS1, P-PI3K, PI3K, AKT and P-AKT expression were detected by Western blot analysis in the liver tissue of T2DM patient and normal human subjects (n=3 in each group). GAPDH was used as the internal control. B. The quantification of IRS1 expression. C. The quantification of P-PI3K expression. D. The quantification of P-AKT expression. *P < 0.05 and **P < 0.01

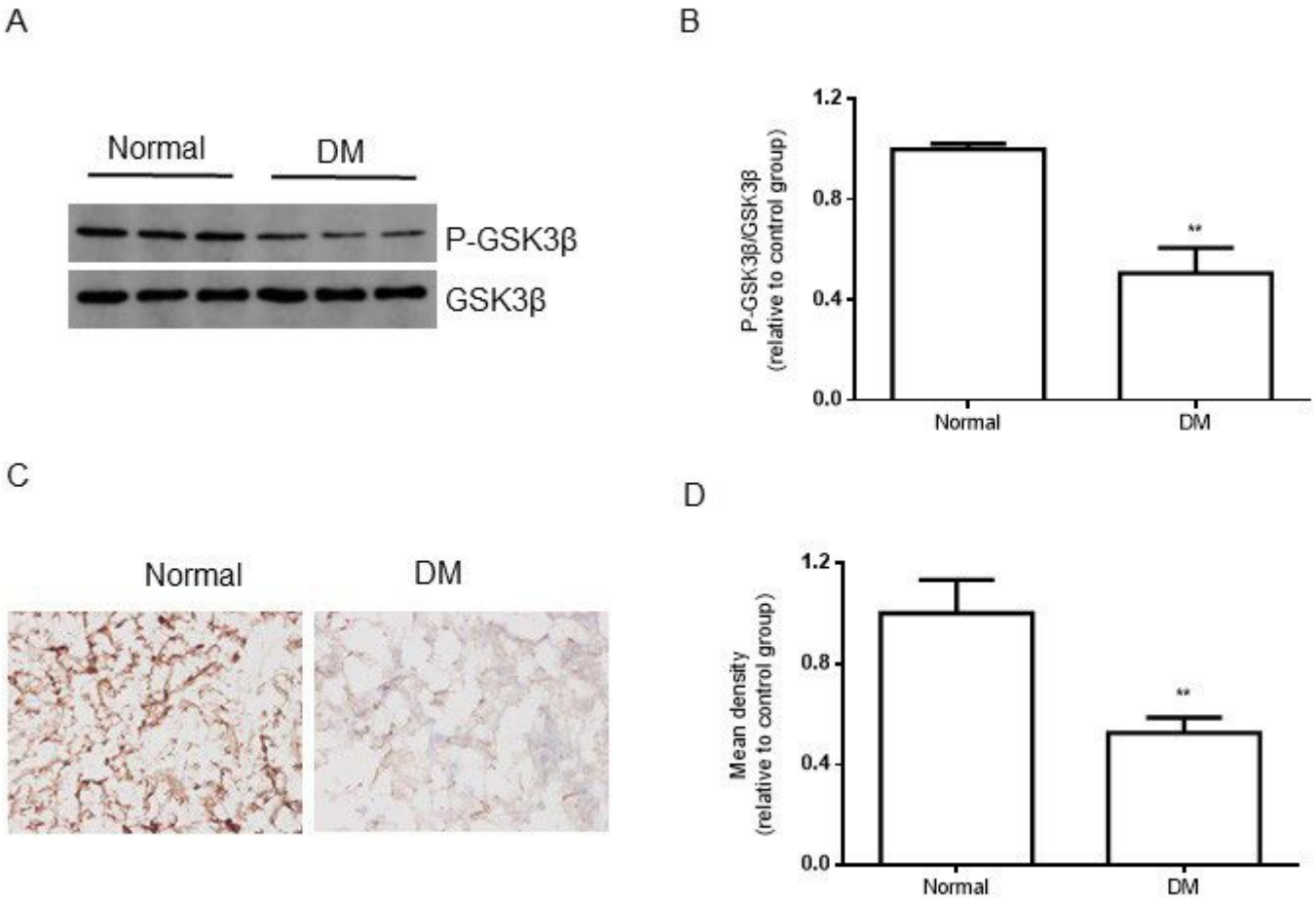


## Figure 3

The expression levels of GSK3β, P-GSK3β and GS in the liver tissue of T2DM patient and normal human subjects. A. Western blot analysis was used to examine the levels of GSK3β and P-GSK3βexpression in the liver tissue of T2DM patient and normal human subjects (n=3 in each group). GAPDH was used as the internal control. B. The quantification of P-GSK3β expression. C. Immunohistochemistry staining was used to examine the level of GS expression in the liver tissue of T2DM patient and normal human subjects (n=3 in each group). D. The quantification of GS expression. **P < 0.01

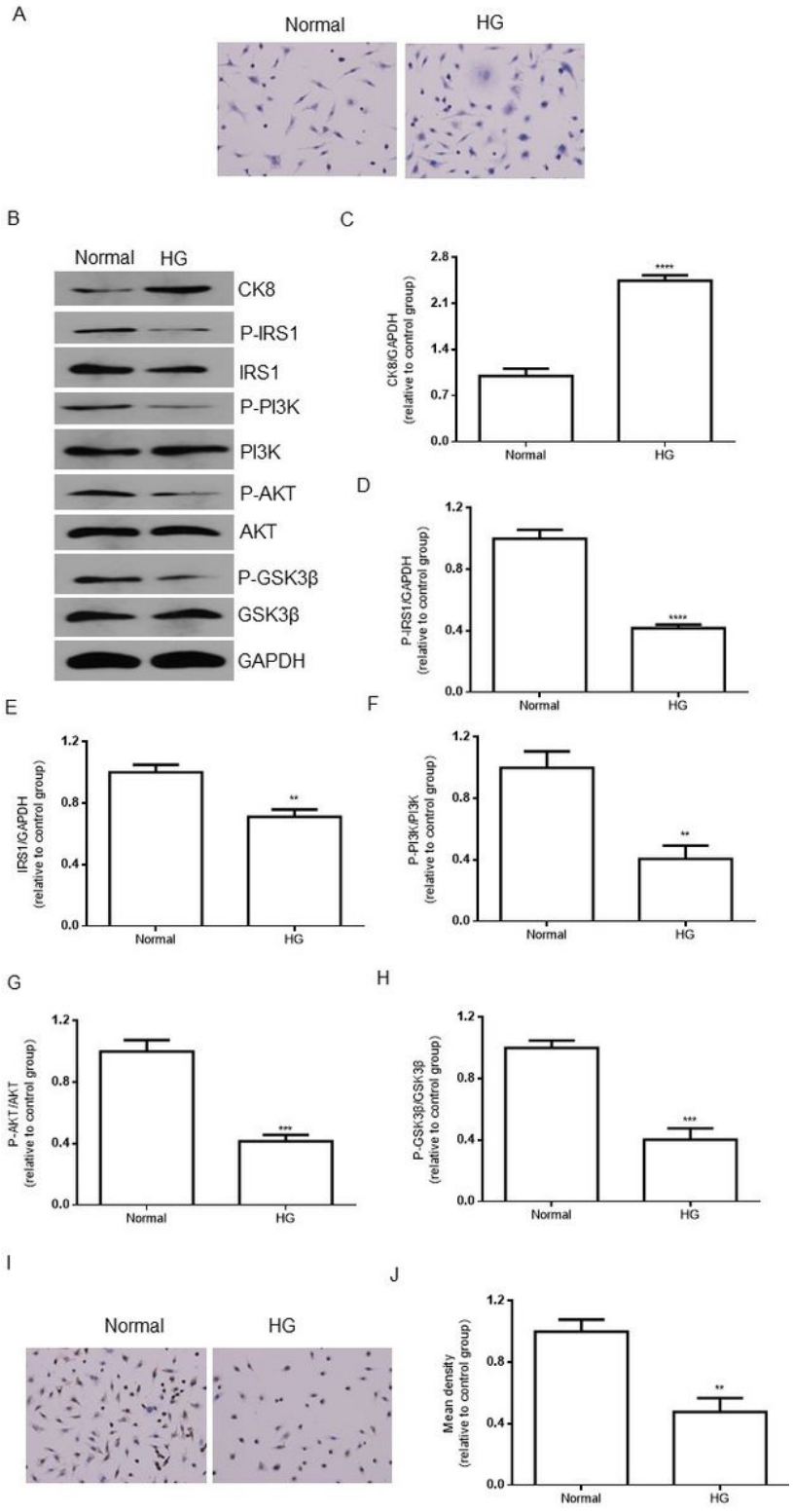


## Figure 4

The effects of high-glucose on glycogen synthesis, CK8 expression and IRS1/PI3K/AKT pathway in liver cell line NCTC1469. NCTC1469 cells were incubated in normal glucose (5.5 m mmol/L) or high glucose (33.3 mmol/L) for 24 h. A. The glycogen content was performed by PAS staining in NCTC1469 cells. B. The expression levels of CK8, IRS1, P-IRS1, P-PI3K, PI3K, AKT, P-AKT, P-GSK3β and GSK3β were detected by Western blot analysis in NCTC1469 cells. GAPDH was used as the internal control. C. The

quantification of CK8 expression. D. The quantification of P-IRS1 expression. E. The quantification of IRS1 expression. F. The quantification of P-PI3K expression. G. The quantification of P-AKT expression. H. The quantification of P-GSK3β expression. I. Immunohistochemistry staining was used to examined the level of GS expression in NCTC1469 cells. J. The quantification of GS expression. *P < 0.05, **P < 0.01, ***P < 0.001 and ****P < 0.0001

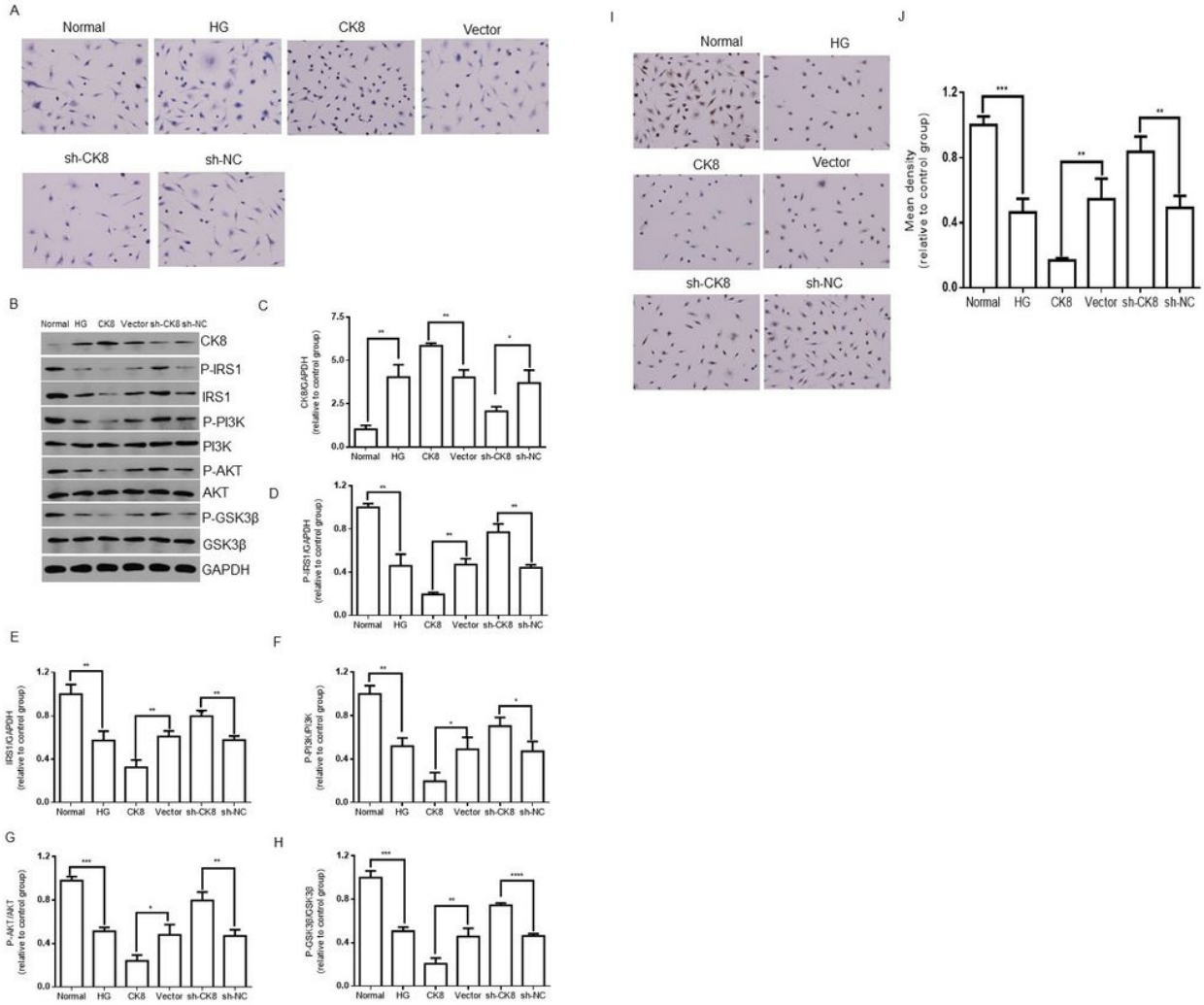


## Figure 5

The effects of CK8 on glycogen synthesis and IRS1/PI3K/AKT pathway in liver cell line NCTC1469. NCTC1469 cells were transfected with empty vector, CK8, sh-NC and sh-CK8 for 24 h, and then NCTC1469 cells were cultured in normal glucose (5.5 m mmol/L) or high glucose (33.3 mmol/L) for 24 h. A. The glycogen content was performed by PAS staining in NCTC1469 cells. B. The expression levels of CK8, IRS1, P-IRS1, P-PI3K, PI3K, AKT, P-AKT, P-GSK3β and GSK3β were detected by Western blot analysis in NCTC1469 cells. GAPDH was used as the internal control. C. The quantification of CK8 expression. D. The

quantification of P-IRS1 expression. E. The quantification of IRS1 expression. F. The quantification of P-PI3K expression. G. The quantification of P-AKT expression. H. The quantification of P-GSK3β expression. I. Immunohistochemistry staining was used to examined the level of GS expression in NCTC1469 cells. J. The quantification of GS expression. *P < 0.05, **P < 0.01, ***P < 0.001 and ****P < 0.0001

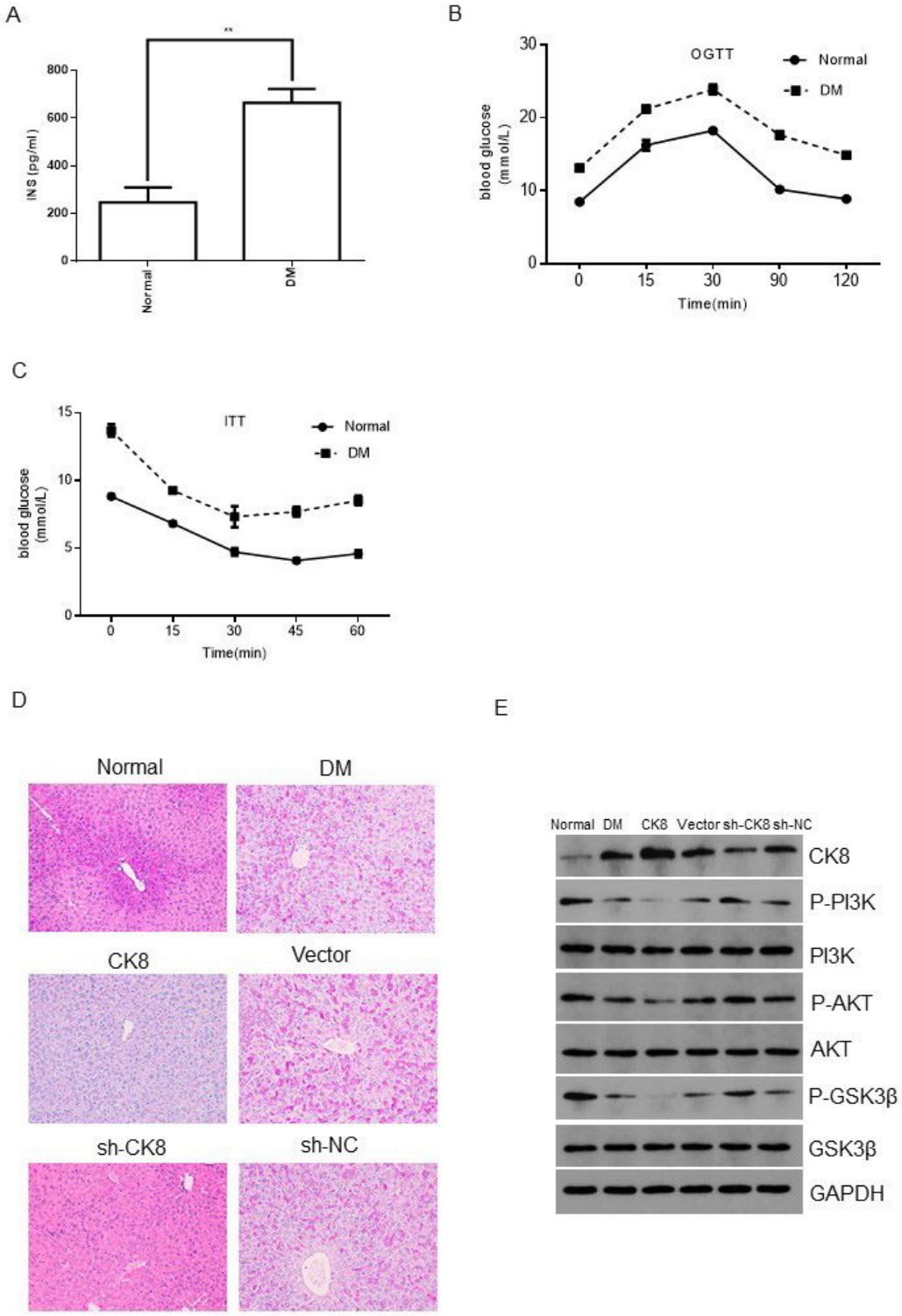


**Figure 6**

The effects of CK8 on glycogen synthesis and PI3K/AKT pathway in vivo. The T2DM mice were transfected with empty vector, CK8, sh-NC and sh-CK8 and fed with high-fat diets for 12 weeks, and then mice were injected with 30 mg/kg STZ. normal mice were fed with normal diets for 12 weeks, and then was injected with a buffer solution for four days in a row. A. The insulin level of the blood serum was detected by using ELISA assay in T2DM mice and normal mice (n=3 in each group). B. The glucose level of blood was detected by OGTT in T2DM mice and normal mice (n=3 in each group). C. The glucose level of blood was detected by ITT in T2DM mice and normal mice (n=3 in each group). D. The liver glycogen content was performed by PAS staining in the liver tissue of T2DM mice and normal mice (n=3 in each group). E. The expression levels of CK8, P-PI3K, PI3K, AKT, P-AKT, P-GSK3β and GSK3β were detected by Western blot analysis in the liver tissue of T2DM mice and normal mice (n=3 in each group). GAPDH was used as the internal control. **P < 0.01.